

Geophysical Research Letters[®]



RESEARCH LETTER

10.1029/2023GL105893

Morphometry of Tidal Meander Cutoffs Indicates Similarity to Fluvial Morphodynamics

Key Points:

- Tidal meander cutoffs are far more common than typically thought and share remarkable morphometric similarities with fluvial counterparts
- Similar mechanisms trigger cutoffs in both tidal and fluvial landscapes, with differences arising only during post-cutoff evolution
- Tidal cutoffs seldom disconnect from parent channels and rarely form oxbows due to the high hydrological connectivity of tidal wetlands

C. Gao^{1,2}, E. D. Lazarus³ , A. D'Alpaos² , M. Ghinassi², A. Ielpi⁴ , G. Parker^{5,6} , A. Rinaldo^{7,8} , P. Gao⁹ , Y. P. Wang^{1,10} , D. Tognin⁷ , and A. Finotello² 

¹Ministry of Education Key Laboratory for Coast and Island Development, School of Geographic and Oceanographic Sciences, Nanjing University, Nanjing, China, ²Department of Geosciences, University of Padova, Padova, Italy, ³School of Geography & Environmental Science, University of Southampton, Southampton, UK, ⁴Department of Earth, Environmental and Geographic Sciences, University of British Columbia-Okanagan, Kelowna, BC, Canada, ⁵Department of Civil & Environmental Engineering, University of Illinois, Urbana, IL, USA, ⁶Department of Geology, University of Illinois, Urbana, IL, USA, ⁷Department of Civil, Environmental, and Architectural Engineering, University of Padova, Padova, Italy, ⁸Laboratory of Ecohydrology, Ecole Polytechnique Federale Lausanne, Lausanne, Switzerland, ⁹Department of Geography and the Environment, Syracuse University, Syracuse, NY, USA, ¹⁰State Key Laboratory of Estuarine and Coastal Research, School of Marine Sciences, East China Normal University, Shanghai, China

Supporting Information:

Supporting Information may be found in the online version of this article.

Correspondence to:

A. Finotello,
alvise.finotello@unipd.it

Citation:

Gao, C., Lazarus, E. D., D'Alpaos, A., Ghinassi, M., Ielpi, A., Parker, G., et al. (2024). Morphometry of tidal meander cutoffs indicates similarity to fluvial morphodynamics. *Geophysical Research Letters*, *51*, e2023GL105893. <https://doi.org/10.1029/2023GL105893>

Received 28 AUG 2023

Accepted 21 DEC 2023

Author Contributions:

Conceptualization: E. D. Lazarus, G. Parker, A. Rinaldo, A. Finotello
Data curation: C. Gao, A. Finotello
Formal analysis: C. Gao, A. Ielpi, A. Finotello
Funding acquisition: A. D'Alpaos, M. Ghinassi, Y. P. Wang, A. Finotello
Investigation: C. Gao, A. Finotello
Methodology: A. D'Alpaos, M. Ghinassi, A. Finotello
Project Administration: A. D'Alpaos, M. Ghinassi, Y. P. Wang
Resources: A. D'Alpaos, M. Ghinassi, Y. P. Wang, A. Finotello

Abstract Sinuous channels wandering through coastal wetlands have been thought to lack lateral-migration features like meander cutoffs and oxbows, spurring the broad interpretation that tidal and fluvial meanders differ morphodynamically. Motivated by recent work showing similarities in planform dynamics between tidal and fluvial meandering channels, we analyzed meander neck cutoffs from diverse tidal and fluvial environments worldwide, and show that tidal cutoffs are widespread. Their perceived paucity stems from pronounced channel density and hydrological connectivity in coastal wetlands, comparatively small size of most tidal channels, and typically dense vegetation cover. Although these factors do not efface tidal meander cutoffs, they collectively inhibit oxbow formation and make tidal cutoffs ephemeral features that can escape detection. We argue that similar morphodynamic processes drive cutoff formation in tidal and fluvial landscapes, with differences arising only during post-cutoff evolution. Such process similarity has important implications for understanding coastal wetland ecomorphodynamics and predicting their long-term evolution.

Plain Language Summary The sinuous channels that wander through tidal coastal wetlands look like meandering rivers. However, features of alluvial floodplains that indicate active river meandering over time, such as oxbow lakes and meander cutoffs, are difficult to find in tidal settings. Their apparent absence has led researchers to infer that tidal and fluvial meanders evolve differently. We re-examined this inference by identifying, measuring, and compiling examples of meander cutoffs from a variety of tidal coastal wetlands and fluvial floodplains worldwide. Our analysis suggests that the shapes and geometric properties of tidal and fluvial cutoffs are indeed remarkably similar. This indicates that while tidal and fluvial environments differ in many ways, they nevertheless share the same physical mechanism affecting meander morphodynamical evolution. Differences between tidal and fluvial meanders do arise after a meander is cut off. We observe that tidal meanders remain preferentially connected to the parent channel, preventing the formation of crescent-shaped oxbow lakes and thus making tidal cutoffs more difficult to detect. Our results indicate a close similarity in meandering channel behavior across tidal and fluvial systems, which opens new opportunities for how researchers model tidal wetlands, with important implications for the effective conservation and restoration of these critical ecosystems.

1. Introduction

Sinuous meandering channels are common in fluvial and coastal landscapes (Leopold et al., 1964). Meandering channels migrate laterally through erosion and deposition of sediment along the outer and inner banks, respectively, of individual meander bends. As meanders evolve, channels frequently shortcut themselves through cutoffs and form oxbow lakes (hereinafter “oxbows”; Dunne & Aalto, 2013; Schwenk et al., 2015; Stølum, 1996). Cutoffs, by which oxbows are formed (Dieras, 2013; Thomas et al., 2022) reduce channel sinuosity, modify rates of lateral migration, and affect floodplain sedimentology, stratigraphy, and sediment residence times (Camporeale et al., 2005; Howard & Hemberger, 1991; Zinger et al., 2011). These dynamics have broad implications for the

© 2024 The Authors.

This is an open access article under the terms of the [Creative Commons Attribution-NonCommercial License](https://creativecommons.org/licenses/by/4.0/), which permits use, distribution and reproduction in any medium, provided the original work is properly cited and is not used for commercial purposes.

Software: A. Finotello
Supervision: A. D'Alpaos, M. Ghinassi, Y. P. Wang, A. Finotello
Validation: C. Gao, A. Finotello
Visualization: C. Gao, A. Finotello
Writing – original draft: C. Gao, E. D. Lazarus, A. Finotello
Writing – review & editing: C. Gao, E. D. Lazarus, A. D'Alpaos, M. Ghinassi, A. Ielpi, G. Parker, A. Rinaldo, P. Gao, Y. P. Wang, D. Tognin, A. Finotello

flux, storage, and sequestration of soil organic carbon (Torres et al., 2017). Meandering river floodplains feature visible evidence of meander migration such as scroll bars and oxbows (Constantine & Dunne, 2008; Dunne & Aalto, 2013; Hooke, 2013). In contrast, channels in tidal coastal floodplains have been thought to lack meander cutoffs, indicating an absence of active meandering (Gabet, 1998; Johnson, 1929) (Figure 1). The perceived stability of sinuous tidal channels—or at least the relative subtlety of their meandering dynamics—has often been attributed to the unique ecomorphodynamics of coastal environments, where flow bidirectionality is paramount (Fagherazzi et al., 2004; Hughes, 2012; Solari et al., 2002). However, recent studies highlighted morphodynamic commonalities between fluvial and tidal meanders, with similar planform dynamics, width-adjusted migration rates, and morphodynamic regimes in high-amplitude bends (Finotello et al., 2018, 2022; Gao, Finotello, & Wang, 2022; Leuven et al., 2016, 2018). This motivated us to question the perceived paucity of tidal meander cutoffs, and to further demonstrate the parallels between tidal and fluvial meandering channels. Here, we analyzed the planform geometry of 600 tidal meander cutoffs identified in high-resolution satellite images from settings around the world, characterized by different tidal regimes, vegetation cover, and geomorphological backgrounds. We conducted a direct comparison with 158 cutoffs in meandering rivers, uncovering striking geometric parallels. These similarities, supported by theoretical, numerical, and field research, suggest a fundamental commonality in morphodynamics across both tidal and fluvial domains.

2. Material and Methods

2.1. Data Collection

We used high-resolution satellite images, freely available from Google Earth Pro, to detect instances of meander cutoffs undisturbed by anthropic activities. These cutoffs, selected for their geographical diversity, span coastal zones and inland alluvial plains across varied climatic and geological settings. Thus, the sampled cutoffs reflect a range of hydrological and tidal regimes, sediment grain sizes, vegetation types, and land cover (Figures 1a–1g). Our full data set includes over 1,200 examples of tidal cutoffs. Of these 1,200 examples, 600 tidal cutoffs with clearly discernible boundaries were manually digitized as polygons using Google Earth Pro. The remainder lacked sufficient detail to be digitized due to poor preservation, dense vegetation canopy, low image resolution, complex morphology resulting from multiple cutoffs, or combinations of these factors, and were categorized as “unanalyzed cases” (Gao & Finotello, 2023). Furthermore, we obtained an additional set of 158 fluvial cutoffs specifically digitized for comparative analyses. These cutoffs were extracted from rivers located in various regions, including the Amazon Basin, the conterminous USA and Alaska, Russia, Canada, Kazakhstan, and New Zealand. The selection was made to ensure a diverse range of channel sizes, with river widths spanning approximately four orders of magnitude (Figure 2).

Tidal cutoffs were also further classified based on several criteria: tidal regime (microtidal $n = 315$; mesotidal $n = 249$; macrotidal $n = 36$), vegetation cover (mangroves $n = 118$; salt marshes $n = 433$; tidal flats $n = 49$), and geomorphological setting (bays $n = 164$; back-barrier lagoons $n = 219$; open coasts $n = 105$; estuaries $n = 112$) (Figure S1 in Supporting Information S1). The mean tidal range (MTR) at each site was determined by analyzing tidal gauge data from Dong (2020) and the National Oceanic and Atmospheric Administration (<https://tidesand-currents.noaa.gov/>), and individual study cases were classified as macro-tidal (MTR > 4 m), meso-tidal (2 < MTR < 4 m), and microtidal (MTR < 2 m).

We focus only on “neck” cutoffs, formed when a high-amplitude loop gets isolated by the pinching connection of two adjacent bends. In the tidal settings we examined, we found no “chute” cutoffs, which are formed when a river bend is shortcut by a new channel cutting through meander point bars—and possibly observed in large, sand-bedded, multi-thread estuarine channels (Leuven et al., 2016).

2.2. Data Analysis

To calculate their morphometric parameters, cutoff polygons were projected into appropriate Universal Transverse Mercator (UTM) coordinates and converted to binary images. The channel centerline was computed based on a standard skeletonization procedure and then resampled using standard cubic spline-fit polylines. Cutoff endpoints were determined as the two branchpoints of the polygon skeleton (Figure 11). To further quantify cutoff planform features, we computed the curvature C ($\text{[m}^{-1}\text{]}$) of the channel centerline as $C = -d\theta/ds$, where θ is the angle between the tangent to the channel axis and an arbitrarily selected reference direction, $x(s)$ and $y(s)$ are the

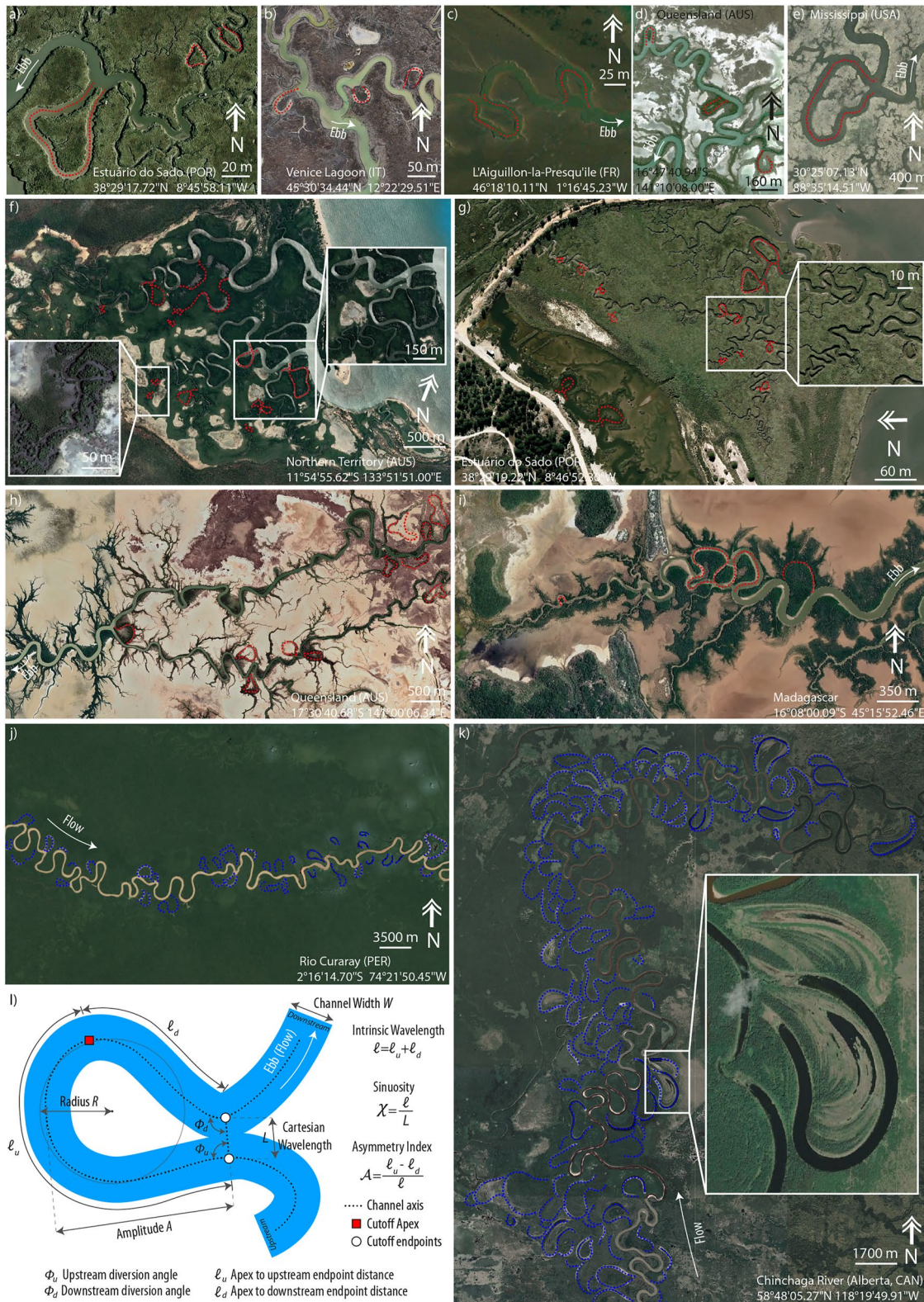


Figure 1. Meander cutoffs in tidal and fluvial landscapes. (a–d) Examples of individual tidal meander cutoffs from distinct coastal settings worldwide (image© Google, Maxar). (f–i) Examples of tidal environments characterized by widespread meander cutoffs (image©Google: TerraMetrics, CNES/Airbus, Maxar, Landsat/ Copernicus). (j, k) Examples of river floodplains littered by oxbow lakes and cutoff traces (image©Google: Maxar). Geographic coordinates are reported in each panel. Dotted red and blue lines highlight discernible traces of meander cutoffs in tidal and fluvial landscapes, respectively. (l) Sketch illustrating the main morphometric features of meander cutoffs analyzed in this study.

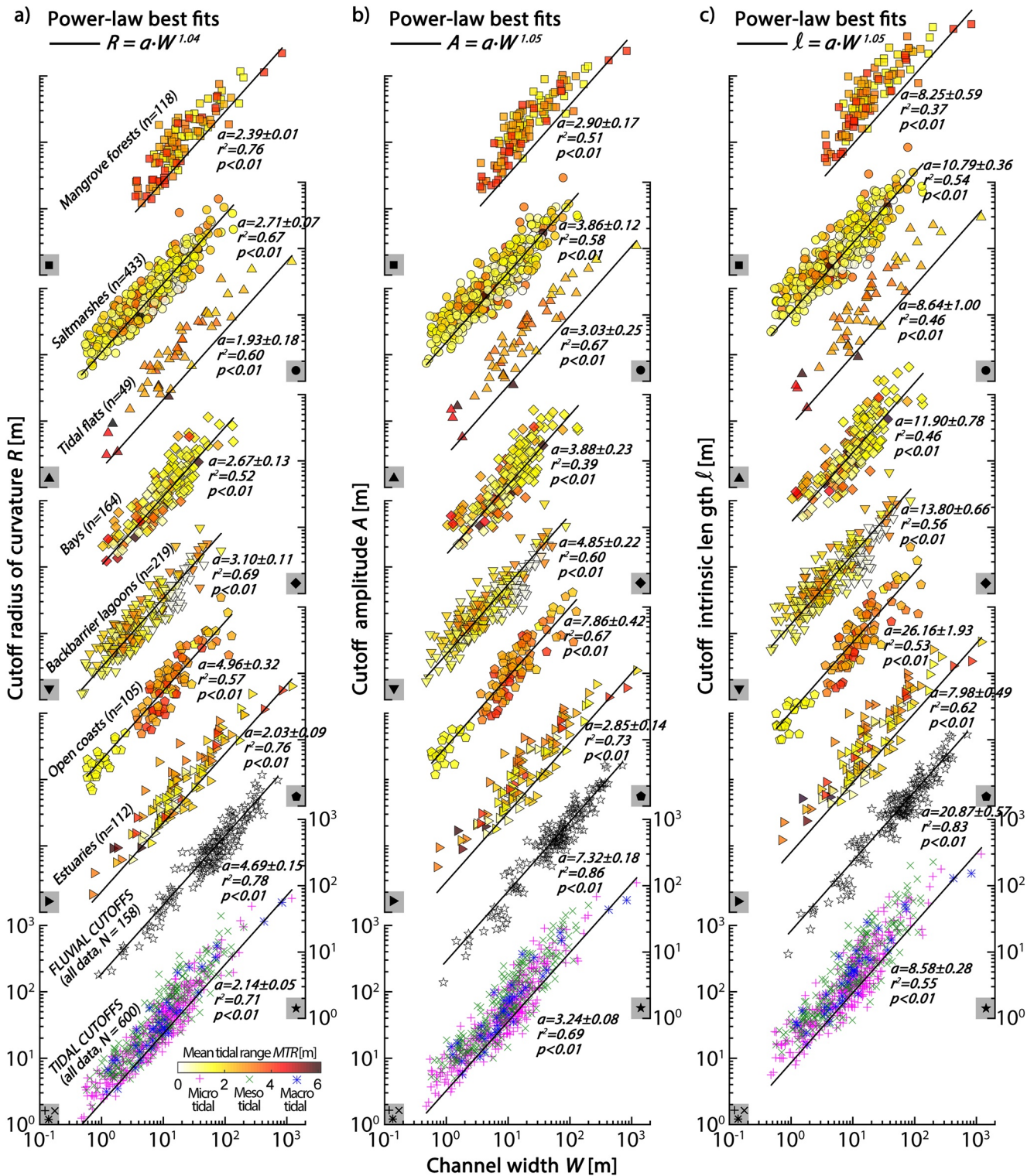


Figure 2. Cutoff morphometrics. Cutoff radius of curvature (R), Amplitude (A), and intrinsic length (l) are plotted against channel width (W) both separately for all tidal and fluvial cutoffs on record and for different tidal-cutoff ensembles based on geomorphological settings and vegetation cover color-coded based on tidal ranges. Continuous black lines represent best-fit power law regressions obtained for different data ensembles, using a common exponent derived from all data and applied to calculate scaling coefficients for each ensemble. Note that the vertical offset among individual data plots is arbitrary: each vertical y-axis ranges from 10^0 to 10^3 , and symbols are positioned at the bottom of the axis to aid in identifying the corresponding data plot.

Cartesian coordinates of a given centerline point, and s is the intrinsic (i.e., along-channel) coordinate, assumed to be positive in the upstream (i.e., landward) direction. Because flow orientation within tidal meanders changes with tidal phases, we hereinafter assume a river-like reference system in which the terms “upstream” and “downstream” refer to landward and seaward directions, respectively.

After computing curvature, a Savitzky–Golay low-pass filter was applied to smooth noise in the original signal. Then, the apex of any individual cutoff was identified as the locus of maximum curvature (Figure 11), and the cutoff asymmetry index was computed as $\mathcal{A} = (\ell_u - \ell_d)/(\ell_u + \ell_d)$ ([-]) where ℓ_u and ℓ_d are the distances between the cutoff apex and its upstream and downstream endpoints, respectively (Figure 11). Negative values of \mathcal{A} correspond to upstream-skewed cutoffs, and positive values of \mathcal{A} to downstream-skewed cutoffs. Other morphometric parameters were also calculated, including: average channel width $y(s)$ ([m]); cutoff intrinsic length $\ell = \ell_u + \ell_d$ ([m]); cutoff cartesian length L ([m]), which is the planar distance between cutoff endpoints; cutoff sinuosity $\chi = \ell/L$ ([-]); cutoff amplitude A ([m]), computed as the maximum point-line distance between the cutoff centerline and the line connecting the two cutoff endpoints; cutoff radius of curvature R ([m]), defined as the radius of the best-fitting circle through all cutoff axis points; and flow-diversion angle ϕ between the cutoff and its parent channel (Figure 11). Because of bidirectional flow through tidal channels, morphodynamically meaningful flow-diversion angles can be identified at both the cutoff upstream (ϕ_u) and downstream (ϕ_d) ends. By comparison, because of the unidirectional flow through river channels, only the upstream flow-diversion angle (ϕ_u) is morphodynamically meaningful for fluvial cutoffs (Dieras, 2013).

To directly compare meander cutoffs of different sizes, dimensional morphometric variables were normalized using channel width (W), such that width-adjusted cutoff radius of curvature, amplitude, and lengths are defined as $R^* = R/W$, $A^* = A/W$, $L^* = L/W$, and $\ell^* = \ell/W$.

3. Results

Dimensional morphometrics— R , A , and ℓ —all exhibit statistically significant power-law relationships to cutoff width W (p -value < 0.01) with matching best-fit power-law exponents and limited separation in power-law scaling constants (Figure 2 and Figure S2 in Supporting Information S1). We also found a statistically significant quasi-linear relation between L and W (Figure S3 in Supporting Information S1), with $L \cong W$. The latter has been described previously as the condition leading to neck cutoff (Li et al., 2022), whereas $L < W$ represents a geometrically impossible configuration (Hayden et al., 2021). Similarly, radius of curvature $R = W/2$ represents a physically meaningful lower bound, since the edges of a channel centerline with a radius of curvature smaller than half its width would intersect each other (Hayden et al., 2021). Although theoretically there are no physical limits to the development of both A and ℓ (besides the basic requirements that $A > 0$ and $\ell > L$ in order for a centerline to be sinuous), the prevalence of smaller curves weights the distribution of meander features toward the physically meaningful lower bound (Vermeulen et al., 2016). For these reasons, the scaling similarity in dimensional metrics reported in Figure 2 is likely due to the finite-width nature of the sinuous features we measured, rather than representing a suitable diagnostic with which to distinguish the fluvial or tidal nature of meander cutoffs. Indeed, previous studies suggest that dimensionless meander morphometrics should be used to infer morphological similarity (Frascati & Lanzoni, 2009; Howard & Hemberger, 1991). We thus performed Kolmogorov–Smirnov tests ($\alpha = 0.05$) on dimensionless morphometric descriptors to highlight that tidal cutoffs are typically less sinuous (i.e., lower χ) and feature smaller width-adjusted radii (R^*), amplitudes (A^*), and intrinsic lengths (ℓ^*) (Figure 3 and Table S1 in Supporting Information S1).

Since meander size and sinuosity are expected to increase with time, our findings indicate that tidal cutoffs are less morphodynamically mature (i.e., less sinuous and planimetrically complex) than their fluvial counterparts. This points to an overall faster evolutionary trajectory from meander inception to cutoffs in tidal settings. However, similar width-adjusted meander migration rates in tidal and fluvial settings (Finotello et al., 2018) contrast with such an interpretation. Furthermore, KS tests demonstrate similar values of asymmetry (\mathcal{A}) and upstream flow-diversion angle (ϕ_u) in tidal and fluvial cutoffs (Figure 3 and Table S1 in Supporting Information S1). Given that neither of these parameters are affected by meander size, the observed similarity not only reflects similar morphodynamic maturity but also suggest shared cutoff-triggering mechanisms, likely associated with the planform configuration of the parent channel (Dieras, 2013). Notably, both fluvial and tidal cutoffs exhibit negative median and peak values of the asymmetry index \mathcal{A} (Figure 3e). That is, both types of cutoffs tend to be upstream-skewed, supporting similarity in their dominant morphodynamic regime (*sensu* Seminara

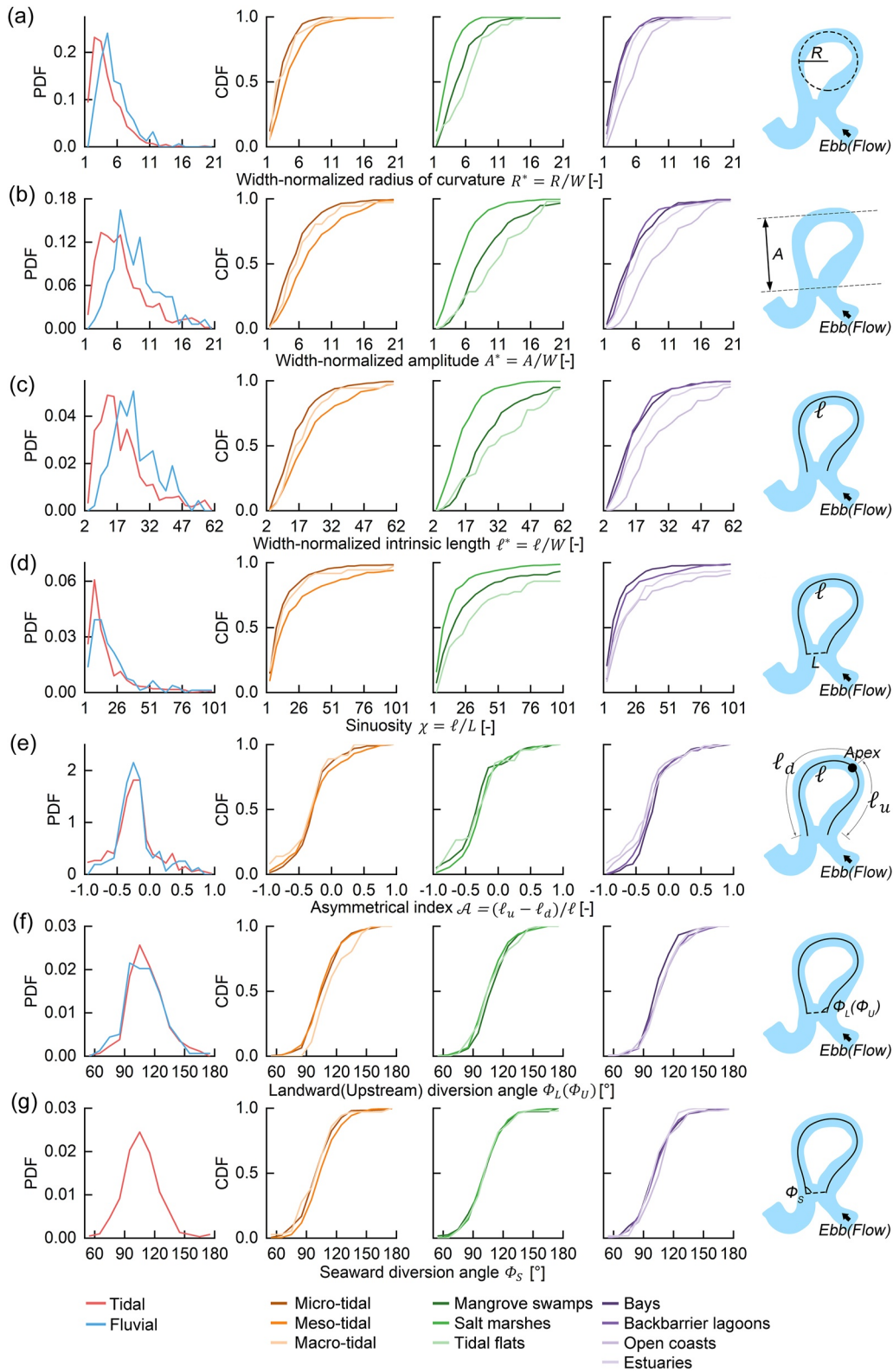


Figure 3. Dimensionless cutoff morphometrics. (a) Width-adjusted radius of curvature (R^*); (b) width-adjusted amplitude (A^*); (c) width-adjusted intrinsic length (ℓ^*); (d) sinuosity (χ); (e) asymmetry index (\mathcal{A}); (f, g) upstream and downstream flow-diversion angles (ϕ_u and ϕ_d). Panels in the first column show empirical probability distributions for tidal (red) and fluvial (blue) cutoffs. Panels in the other columns report empirical cumulative frequency distributions for tidal cutoffs subdivided based on tidal range, vegetation cover, and geomorphological setting. The fifth column contains sketch-up views for each investigated morphometric.

et al., 2001). This observation likely stems from the morphodynamic dominance, in tidal channels, of either flood or (more commonly) ebb flows that effectively render tidal meanders similar to their fluvial counterparts featuring unidirectional flows (Fagherazzi et al., 2004; Kleinhans et al., 2009).

We propose that the comparatively smaller size of tidal cutoffs, relative to fluvial ones, is not a result of fundamental differences in their morphodynamics. Instead, it appears to be predominantly influenced by the specific hydrological, ecological, and geomorphological attributes inherent to tidal wetlands. Specifically, we hypothesize that the dense distribution of tidal channels that typically characterizes tidal wetlands accounts for the reduced size and sinuosity of tidal cutoffs, with enhanced hydrological connectivity explaining the apparent paucity of cutoff traces in tidal environments as we discuss below.

4. Discussion

4.1. Dense Channel Distribution Limits Stream Meandering and Cutoff Formation

Meander migration in densely channeled tidal floodplains shapes the landscape differently than in fluvial contexts, where rivers can freely migrate laterally without intercepting other channels and confluences are comparatively infrequent. Tidal wetlands are characterized by high drainage density—taken as the mean shortest distance that a parcel of water placed on the wetland surface would need to travel before reaching the closest channel (Marani et al., 2003). Such enhanced drainage density limits meander dynamics by preventing channels from freely migrating and meanders from fully developing without intercepting adjoining streams (Letzsch & Frey, 1980; Vilas et al., 1999). A similar dynamic is described in multi-thread, anabranching rivers with individual sinuous anabranches, where enhanced channel density limits cutoff formation (Schumm et al., 1996). Accordingly, evidence from modern and ancient deposits shows that channel piracy (i.e., stream captures) in dense tidal networks (Figure S4 in Supporting Information S1) limit the lateral accretion of point bar bodies and can modify the network-scale distribution of the tidal prism, feeding back into the long term ecomorphodynamic evolution of the entire tidal system (Cosma et al., 2020; Finotello, Ghinassi, et al., 2020). Hence, enhanced channel density limits tidal meander dynamics and cutoff formation.

Our hypothesis is further corroborated by systematic statistically significant differences observed in the distributions of R^* , A^* , L^* , and χ as a function of vegetation cover, with effects of tidal regime and geomorphological background being significant but less systematic (Figure 3 and Tables S2–S13 in Supporting Information S1). Tidal cutoffs in salt marshes are smaller and less sinuous than those found in mangrove forests and tidal flats (Figure 3).

This trend resonates with existing research indicating that tidal channel networks are denser in vegetated areas, especially in salt marshes (Kearney & Fagherazzi, 2016; Schwarz et al., 2022).

This evidence supports our contention that in densely channelized tidal wetlands, meander cutoffs are constrained in their size and sinuosity growth due to the increased likelihood of channel piracy during lateral migration. Similar cutoff asymmetries (\mathcal{A}) and flow-diversion angles (ϕ_u , ϕ_d) among distinct tidal settings also support similarity in the morphodynamic processes responsible for cutoff development. Kolmogorov-Smirnov tests reveal significant differences in the distributions of ϕ_u , ϕ_d , and \mathcal{A} only based on geomorphological setting (Tables S2–S13 in Supporting Information S1), but we find no differences in these morphometrics as a function of tidal range and vegetation cover despite the potential influence that both controls can exert on channel bank erosion (Gao, Finotello, D'Alpaos, et al., 2022; Gasparotto et al., 2022; Zhao et al., 2022).

4.2. Hydrological Connectivity Control on Post-Cutoff Development

To further substantiate that differences in tidal and fluvial cutoff morphology do not stem from dissimilarities in meander morphodynamics, we also examined the connection state of individual cutoffs with their parent channels. Once a river meander is cut off, a plug bar forms in response to flow separation and reduced energy conditions, leading to the rapid deposition of coarse sediment and blockage of both cutoff entrances (Toonen et al., 2012). Eventually, the cutoff becomes completely disconnected from the parent channel and forms an oxbow. Based on the presence and position of plug bars in our tidal and fluvial examples, we classified cutoffs into four groups: completely connected, upstream connected, downstream connected, and disconnected (Figure 4). The upstream- and downstream-connected cases can also be merged into a broader category of partially connected cutoffs.

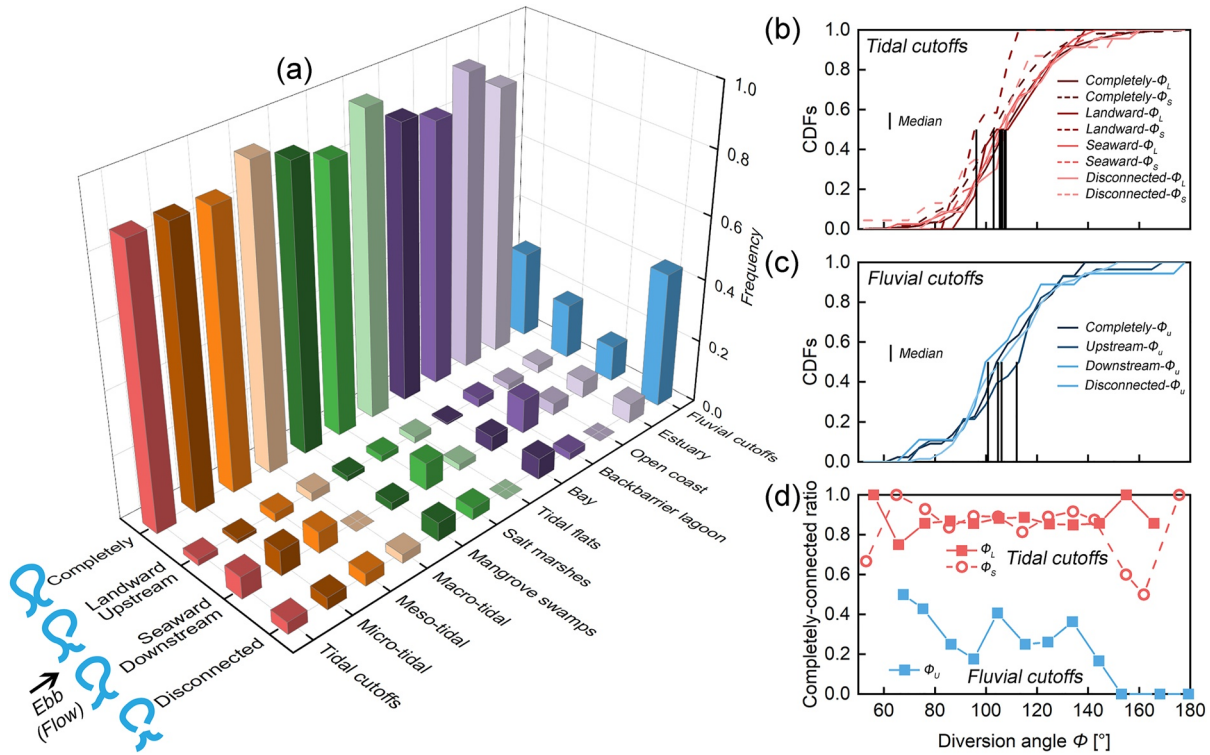


Figure 4. Cutoff connectivity. (a) Barplot showing the relative frequency of different connection types between cutoffs and parent channels, differentiating tidal (red) and fluvial (blue) cutoffs, and further segmenting tidal cutoff ensemble based on tidal range (orange), vegetation cover (green), and geomorphological settings (purple). (b, c) Frequency distributions of flow-diversion angles (ϕ) for tidal and fluvial cutoffs. Different colors denote different connectivity with the parent channel. Solid and dashed lines denote upstream and downstream diversion angles, respectively. (d) Share of completely connected tidal (red) and fluvial (blue) cutoffs across uniform 10° diversion-angle intervals. Solid squares and empty dots denote upstream and downstream diversion angles, respectively. (e) Tidal cutoffs found in the microtidal lagoon of Venice (Italy) characterized by different connectivity.

Whereas more than 43% of fluvial cutoffs in our data set are entirely disconnected and only 28% are completely connected (Figure 4a), tidal cutoffs tend to remain connected to their parent channels, with 87% of examples completely connected, 9% partially connected, and only 4% entirely disconnected (Figure 4a).

This observed distinction in the connection state of tidal versus fluvial cutoffs appears to be independent of factors such as tidal range, vegetation cover, and geomorphological setting (Figure 4). This finding effectively dispels the notion that the absence of plug bars in tidal cutoffs depends on site-specific landscape characteristics (e.g., sediment grain size; Kleinhans et al., 2024).

Moreover, similar flow-diversion angles are observed in all our study cases, with median values consistently ranging between 105° and 108° (Figures 4b and 4c) and further pointing to similar cutoff-triggering mechanisms in fluvial and tidal landscapes. Morphological differences thus can be expected to emerge once cutoffs have formed. The percentage of completely connected fluvial cutoffs decreases as the flow-diversion angle increases, implying that larger ϕ_u promote the formation of plug bars and oxbows (Figure 4d). In contrast, tidal cutoffs tend to remain connected to their parent channel irrespective of flow-diversion angles, whether upstream or downstream (Figure 4d and Figure S5 in Supporting Information S1).

Therefore, unlike fluvial analogs, most tidal cutoffs remain hydrodynamically active to some extent: periodic overbank flows in tidal channels result in significant rates of lateral flow injections from the adjoining tidal floodplains during ebb tide, which maintain active flows even in cutoff bends and prevent plug-bar formation by keeping the cutoff entrance flushed. Notably, some tidal cutoffs may also remain connected to other active parts of the network through minor lateral tributaries flowing directly into the cutoff (Figures 1a–1i and Figure S6 in Supporting Information S1). Hence, pronounced hydrological connectivity in tidal wetlands prevents the formation of plug bars and the subsequent evolution of tidal cutoffs into oxbows. Such an evolutionary trajectory clearly differs from fluvial cutoffs, which are typically abandoned and receive water and sediment input

almost exclusively during major floods either through minor tie channels carved through the plug bar (Rowland et al., 2009) or as the entire alluvial plain floods (Shen et al., 2021).

Among the partially connected cutoffs in our data set, the fluvial ones are preferentially connected with their parent channels at the upstream end: plug bars tend to form at the cutoff downstream end where flow separations and recirculation create a zone of dead velocity that hinders mixing and promotes sediment deposition (e.g., Turnipseed et al., 2021). In contrast, the few partially connected tidal cutoffs on record, tend to maintain connectivity at the downstream end (Figure 4a), aligned with the direction of typically dominant ebb flows that seemingly keep the cutoff downstream end periodically flushed.

4.3. Meander Cutoffs in Tidal Coastal Landscapes: Rare or Everywhere?

Abundant tidal cutoffs akin to oxbow-rich alluvial floodplains can be found in some tidal settings with possibly lower drainage density and/or sediment supply that limits cutoff infill and vegetation encroachment (Figures 1f–1i; Figures S7 and S8 in Supporting Information S1). This further corroborates the observation that tidal and fluvial meandering channels not only evolve through similar morphodynamic processes, but also that tidal meanders are as prone to form cutoffs as their fluvial counterparts given conducive environmental conditions. Given the apparent ubiquity of cutoffs across a variety of tidal environments, why has the notion that sinuous tidal channel bends are inherently unlikely to cut off prevailed for so long (Gabet, 1998; Johnson, 1929)?

We suggest that, first, the characteristic width and amplitude of fluvial cutoffs may not vary significantly along a given reach of a meandering river between major tributaries, whereas meander cutoffs within a given tidal wetland can occur across a broad range of meander wavelengths and widths (Finotello, D'Alpaos, et al., 2020). Low-order, narrow tidal creeks are more frequently found than higher-order, wide channels and are thus the most likely to express cutoff development (Figures 1a–1i; Figures S7 and S8 in Supporting Information S1). Yet small channels produce small cutoffs, which are especially challenging to observe from a broader spatial vantage, particularly when the vegetation canopy is dense (e.g., in mangrove forests, Figure S9 in Supporting Information S1).

Another consideration is the sustained rate of vertical accretion that characterizes tidal wetlands, coupled with halophytic vegetation that can tolerate significant waterlogging stress. These factors may becloud cutoff traces (Figures 1b, 1d, 1f–1i and Figure S9 in Supporting Information S1) through rapid sedimentation in the less hydrodynamically active portions of the cutoff, and the subsequent encroachment of vegetation. This levels out cutoff geomorphic expressions and further hinders their identification from aerial images. Although similar reasoning could apply to fluvial floodplains, reduced overbank sediment supply and slower rates of riparian vegetation growth in permanently waterlogged areas may prolong the timescale required to fill oxbows, making large river-cutoff scars identifiable from aerial photos for much longer periods (Kleinbans et al., 2024) (Figures 1j and 1k).

The apparent absence of tidal cutoffs is thus more an artifact of observations than a consequence of physical mechanisms. High drainage densities in tidal wetlands surely constrain the freely meandering of tidal channels (Figure S10 in Supporting Information S1). Yet the relatively small size of most tidal channels, along with the distinctive hydrological characteristics of tidal wetlands, contribute to the transient nature of tidal cutoffs and make them challenging to record. That is, unlike other features of meandering channels that might jump out at the observer, to find tidal cutoffs one has to go carefully looking for them.

The implied morphodynamic similarity between tidal and fluvial meanders is by no means diminished by the absence of prominent scroll bars in tidal wetlands, standing in stark contrast to river floodplains that often—but not always (Candel et al., 2020, 2021)—showcase intricate arrangements of sub-parallel scrolls indicative of previous channel locations (Figure 1k) (Strick et al., 2018). While there is no consensus on what drives the formation of scroll bars (van de Lageweg et al., 2014), we offer two possible, not mutually exclusive explanations for the absence of scroll bars in tidal meanders. One possibility is that tidal meanders undergo small and yet continuous incremental migrations, unlike fluvial meanders which tend to migrate more episodically during major flood events (Mason & Mohrig, 2019; Wu et al., 2016). Another hypothesis is that sustained rates of vertical aggradation relative to lateral channel migration in tidal wetlands prevent scroll bars by systematically overshadowing any topographic irregularities (Brivio et al., 2016; Cosma et al., 2019). This explanation aligns with the lack of scroll bars in meandering streamflows evolving through curvature-driven fluvial-like mechanisms in

aggradational settings such as coastal backwater areas (Swartz et al., 2020), peatlands (Candel et al., 2017), and submarine turbidity-current channels (Jobe et al., 2016; Morris et al., 2024).

5. Implications and Conclusions

Our findings demonstrate that meandering channels in tidal wetlands possess the same capacity to form meander cutoffs as their fluvial counterparts. The morphometric evidence we have gathered suggests that the morphodynamic processes driving the development of both tidal and fluvial cutoffs are fundamentally similar. However, substantial differences arise after cutoffs have formed. Unlike fluvial cutoffs, which tend to form oxbows, tidal cutoffs remain preferentially connected to their parent channel. This distinction is attributed to the pronounced hydrological connectivity characteristic of tidal wetlands. As a result, tidal meander cutoffs continue to actively participate in the draining and flooding of the surrounding wetlands, and maintain their status as integral components of the overall system.

Considered alongside previous studies, our results indicate a complete morphodynamic analogy between tidal and fluvial meandering channels from meander inception to cutoff (Finotello et al., 2018, 2022; Gao, Finotello, & Wang, 2022; Leuven et al., 2018). The unification of tidal and fluvial meander morphodynamics allows for extending classical techniques for modeling meandering rivers (Bogoni et al., 2017; Howard & Knutson, 1984; Parker et al., 2011; Seminara et al., 2001) to tidal wetland contexts, where meandering is ubiquitous and yet routinely omitted. Such an advance in numerical modeling would open new opportunities for how researchers model tidal wetland ecomorphodynamics, with important implications for the effective conservation and restoration of these critical ecosystems.

Conflict of Interest

The authors declare no conflicts of interest relevant to this study.

Data Availability Statement

All the data presented and analyzed in this paper are freely available from a public Zenodo folder (Gao & Finotello, 2023).

References

- Bogoni, M., Putti, M., & Lanzoni, S. (2017). Modeling meander morphodynamics over self-formed heterogeneous floodplains. *Water Resources Research*, 53(6), 5137–5157. <https://doi.org/10.1002/2017WR020726>
- Brivio, L., Ghinassi, M., D'Alpaos, A., Finotello, A., Fontana, A., Roner, M., & Howes, N. (2016). Aggradation and lateral migration shaping geometry of a tidal point bar: An example from salt marshes of the Northern Venice Lagoon (Italy). *Sedimentary Geology*, 343, 141–155. <https://doi.org/10.1016/j.sedgeo.2016.08.005>
- Camporeale, C., Perona, P., Porporato, A., & Ridolfi, L. (2005). On the long-term behavior of meandering rivers. *Water Resources Research*, 41(12), 1–13. <https://doi.org/10.1029/2005WR004109>
- Candel, J. H. J., Kleinans, M. G., Makaske, B., & Wallinga, J. (2021). Predicting river channel pattern based on stream power, bed material and bank strength. *Progress in Physical Geography*, 45(2), 253–278. <https://doi.org/10.1177/0309133320948831>
- Candel, J. H. J., Makaske, B., Kijm, N., Kleinans, M. G., Storms, J. E. A., & Wallinga, J. (2020). Self-constraining of low-energy rivers explains low channel mobility and tortuous planforms. *Depositional Record*, 6(3), 648–669. <https://doi.org/10.1002/dep2.112>
- Candel, J. H. J., Makaske, B., Storms, J. E. A., & Wallinga, J. (2017). Oblique aggradation: A novel explanation for sinuosity of low-energy streams in peat-filled valley systems. *Earth Surface Processes and Landforms*, 42(15), 2679–2696. <https://doi.org/10.1002/esp.4100>
- Constantine, J. A., & Dunne, T. (2008). Meander cutoff and the controls on the production of oxbow lakes. *Geology*, 36(1), 23–26. <https://doi.org/10.1130/G24130A.1>
- Cosma, M., Finotello, A., Ielpi, A., Ventra, D., Oms, O., D'Alpaos, A., & Ghinassi, M. (2020). Piracy-controlled geometry of tide-dominated point bars: Combined evidence from ancient sedimentary successions and modern channel networks. *Geomorphology*, 370, 107402. <https://doi.org/10.1016/j.geomorph.2020.107402>
- Cosma, M., Ghinassi, M., D'Alpaos, A., Roner, M., Finotello, A., Tommasini, L., & Gatto, R. (2019). Point-bar brink and channel thalweg trajectories depicting interaction between vertical and lateral shifts of microtidal channels in the Venice Lagoon (Italy). *Geomorphology*, 342, 37–50. <https://doi.org/10.1016/j.geomorph.2019.06.009>
- Dieras, P. L. (2013). In *The persistence of oxbow lakes as aquatic habitats: An assessment of rates of change and patterns of alluviation* (doctorate of philosophy) (Vol. 177). Retrieved from <http://orca.cf.ac.uk/49392/>
- Dunne, T., & Aalto, R. E. (2013). Large River floodplains. In J. E. Schroder & E. Wohl (Eds.), *Treatise on geomorphology* (Vol. 9, pp. 645–678). Elsevier. <https://doi.org/10.1016/B978-0-12-374739-6.00258-X>
- Fagherazzi, S., Gabet, E. J., & Furbish, D. J. (2004). The effect of bidirectional flow on tidal channel planforms. *Earth Surface Processes and Landforms*, 29(3), 295–309. <https://doi.org/10.1002/esp.1016>

Acknowledgments

We are grateful for constructive reviews from M. Kleinans and one anonymous reviewer, as well as for recommendations from the Editorial Office, which improved this manuscript. This study is funded by the European Union—NextGenerationEU and by the University of Padua under the 2021 STARS Grants@Unipd programme “TiDyLLy- Tidal networks dynamics as drivers for ecomorphodynamics of low-lying coastal area” (to AF), as well as by a China Scholarship Council (CSC) scholarships (202106190084, to CG). AI is supported by a Discovery Grant from the Natural Sciences and Engineering Research Council of Canada. AF, MG, and ADA also acknowledge support by the Italian Ministry of University and Research (MUR) through the project titled “The Geosciences for Sustainable Development” (Budget MUR—Dipartimenti di Eccellenza 2023–2027; Project ID C93C23002690001).

- Finotello, A., Capperucci, R. M., Bartholomä, A., D'Alpaos, A., & Ghinassi, M. (2022). Morpho-sedimentary evolution of a microtidal meandering channel driven by 130 years of natural and anthropogenic modifications of the Venice Lagoon (Italy). *Earth Surface Processes and Landforms*, *47*(10), 2580–2596. <https://doi.org/10.1002/esp.5396>
- Finotello, A., D'Alpaos, A., Bogoni, M., Ghinassi, M., & Lanzoni, S. (2020). Remotely-sensed planform morphologies reveal fluvial and tidal nature of meandering channels. *Scientific Reports*, *10*(1), 1–13. <https://doi.org/10.1038/s41598-019-56992-w>
- Finotello, A., Ghinassi, M., Carniello, L., Belluco, E., Pivato, M., Tommasini, L., & D'Alpaos, A. (2020). Three-dimensional flow structures and morphodynamic evolution of microtidal meandering channels. *Water Resources Research*, *56*(7), e2020WR027822. <https://doi.org/10.1029/2020WR027822>
- Finotello, A., Lanzoni, S., Ghinassi, M., Marani, M., Rinaldo, A., & D'Alpaos, A. (2018). Field migration rates of tidal meanders recapitulate fluvial morphodynamics. *Proceedings of the National Academy of Sciences of the United States of America*, *115*(7), 1463–1468. <https://doi.org/10.1073/pnas.1711330115>
- Frascati, A., & Lanzoni, S. (2009). Morphodynamic regime and long-term evolution of meandering rivers. *Journal of Geophysical Research*, *114*(2), 1–12. <https://doi.org/10.1029/2008JF001101>
- Gabet, E. J. (1998). Lateral migration and bank erosion in a Saltmarsh tidal channel in San Francisco Bay, California. *Estuaries*, *21*(4), 745. <https://doi.org/10.2307/1353278>
- Gao, C., & Finotello, A. (2023). Morphometry of widespread tidal meander cutoffs discloses similarity to fluvial morphodynamics [Dataset]. Zenodo. <https://doi.org/10.5281/zenodo.8229300>
- Gao, C., Finotello, A., D'Alpaos, A., Ghinassi, M., Carniello, L., Pan, Y., et al. (2022). Hydrodynamics of meander bends in intertidal mudflats: A field study from the macrotidal Yangkou Coast, China. *Water Resources Research*, *58*(12), 1–28. <https://doi.org/10.1029/2022WR033234>
- Gao, C., Finotello, A., & Wang, Y. P. (2022). Predominant landward skewing of tidal meanders. *Earth Surface Processes and Landforms*, *47*(13), 1–17. <https://doi.org/10.1002/esp.5452>
- Gasparotto, A., Darby, S. E., Leyland, J., & Carling, P. A. (2022). Water level fluctuations drive bank instability in a hypertidal estuary. *Earth Surface Dynamics*, *2080*, 1–28.
- Hayden, A. T., Lamb, M. P., & Carney, A. J. (2021). Similar curvature-to-width ratios for channels and channel belts: Implications for paleo-hydraulics of fluvial ridges on Mars. *Geology*, *49*(7), 837–841. <https://doi.org/10.1130/G48370.1>
- Hooke, J. M. (2013). River meandering. In J. E. Schroder & E. Wohl (Eds.), *Treatise on geomorphology* (Vol. 9, pp. 260–288). Elsevier. <https://doi.org/10.1016/B978-0-12-374739-6.00241-4>
- Howard, A. D., & Hemberger, A. T. (1991). Multivariate characterization of meandering. *Geomorphology*, *4*(3–4), 161–186. [https://doi.org/10.1016/0169-555X\(91\)90002-R](https://doi.org/10.1016/0169-555X(91)90002-R)
- Howard, A. D., & Knutson, T. R. (1984). Sufficient conditions for river meandering: A simulation approach. *Water Resources Research*, *20*(11), 1659–1667. <https://doi.org/10.1029/WR020i011p01659>
- Hughes, Z. J. (2012). Tidal channels on tidal flats and marshes. In R. A. Davis & R. W. Dalrymple (Eds.), *Principles of tidal sedimentology* (pp. 269–300). Springer. https://doi.org/10.1007/978-94-007-0123-6_11
- Jobe, Z. R., Howes, N. C., & Auchter, N. C. (2016). Comparing submarine and fluvial channel kinematics: Implications for stratigraphic architecture. *Geology*, *44*(11), 931–934. <https://doi.org/10.1130/G38158.1>
- Johnson, D., & Campbell, M. R. (1929). Meanders in tidal streams: A review and discussion. *Geographical Review*, *19*(1), 135. <https://doi.org/10.2307/208081>
- Kearney, W. S., & Fagherazzi, S. (2016). Salt marsh vegetation promotes efficient tidal channel networks. *Nature Communications*, *7*, 1–7. <https://doi.org/10.1038/ncomms12287>
- Kleinhans, M. G., McMahon, W. J., & Davies, N. S. (2024). What even is a meandering river? A philosophy-enhanced synthesis of multilevel causes and systemic interactions contributing to river meandering. *Geological Society, London, Special Publications*, *540*(1). <https://doi.org/10.1144/sp540-2022-138>
- Kleinhans, M. G., Schuurman, F., Bakx, W., & Markies, H. (2009). Meandering channel dynamics in highly cohesive sediment on an intertidal mud flat in the Westerschelde estuary, The Netherlands. *Geomorphology*, *105*(3–4), 261–276. <https://doi.org/10.1016/j.geomorph.2008.10.005>
- Leopold, L. B., Wolman, M. G., & Miller, J. P. (1964). *Fluvial processes in geomorphology* (Freeman). San Francisco. Retrieved from <http://catalogue.nla.gov.au/Record/2338901>
- Letzsch, W. S., & Frey, R. W. (1980). Deposition and erosion in a holocene salt marsh, Sapelo Island, Georgia. *Journal of Sedimentary Petrology*, *50*(2), 529–542. <https://doi.org/10.1306/212F7A45-2B24-11D7-8648000102C1865D>
- Leuven, J. R. F. W., Kleinhans, M. G., Weisscher, S. A. H., & van der Vegt, M. (2016). Tidal sand bar dimensions and shapes in estuaries. *Earth-Science Reviews*, *161*, 204–223. <https://doi.org/10.1016/j.earscirev.2016.08.004>
- Leuven, J. R. F. W., van Maanen, B., Lexmond, B. R., van der Hoek, B. V., Spruijt, M. J., & Kleinhans, M. G. (2018). Dimensions of fluvial-tidal meanders: Are they disproportionately large? *Geology*, *46*(10), 923–926. <https://doi.org/10.1130/G45144.1>
- Li, Z., Gao, P., You, Y., Finotello, A., & Ielpi, A. (2022). Delayed neck cutoff in the meandering Black River of the Qinghai–Tibet plateau. *Earth Surface Processes and Landforms*, *48*(5), 1–12. <https://doi.org/10.1002/esp.5534>
- Marani, M., Belluco, E., D'Alpaos, A., Defina, A., Lanzoni, S., & Rinaldo, A. (2003). On the drainage density of tidal networks. *Water Resources Research*, *39*(2), 1–11. <https://doi.org/10.1029/2001WR001051>
- Mason, J., & Mohrig, D. (2019). Scroll bars are inner bank levees along meandering river bends. *Earth Surface Processes and Landforms*, *44*(13), 2649–2659. <https://doi.org/10.1002/esp.4690>
- Morris, P. D., Sylvester, Z., Covault, J. A., Mohrig, D., & Dunlap, D. (2024). Fluvial-style migration controls autogenic aggradation in submarine channels: Joshua Channel, eastern Gulf of Mexico. In A. Finotello, Z. Sylvester, & P. R. Durkin (Eds.), *Meandering streamflows: Patterns and processes across landscapes and scales* (Vol. 540). Geological Society, London, Special Publications. <https://doi.org/10.1144/SP540-2022-123>
- Parker, G., Shimizu, Y., Wilkerson, G. V., Eke, E. C., Abad, J. D., Lauer, J. W., et al. (2011). A new framework for modeling the migration of meandering rivers. *Earth Surface Processes and Landforms*, *36*(1), 70–86. <https://doi.org/10.1002/esp.2113>
- Rowland, J. C., Dietrich, W. E., Day, G., & Parker, G. (2009). Formation and maintenance of single-thread tie channels entering floodplain lakes: Observations from three diverse river systems. *Journal of Geophysical Research*, *114*(2), 1–19. <https://doi.org/10.1029/2008JF001073>
- Schumm, S. A., Erskine, W. D., & Tilleard, J. W. (1996). Morphology, hydrology, and evolution of the anastomosing Ovens and King Rivers, Victoria, Australia. *Bulletin of the Geological Society of America*, *108*(10), 1212–1224. [https://doi.org/10.1130/0016-7606\(1996\)108<1212:MHAEOT>2.3.CO;2](https://doi.org/10.1130/0016-7606(1996)108<1212:MHAEOT>2.3.CO;2)
- Schwarz, C., van Rees, F., Xie, D., Kleinhans, M. G., & van Maanen, B. (2022). Salt marshes create more extensive channel networks than mangroves. *Nature Communications*, *13*(1), 2017. <https://doi.org/10.1038/s41467-022-29654-1>
- Schwenk, J., Lanzoni, S., & Foufoula-Georgiou, E. (2015). The life of a meander bend: Connecting shape and dynamics via analysis of a numerical model. *Journal of Geophysical Research: Earth Surface*, *120*(4), 690–710. <https://doi.org/10.1002/2014JF003252>

- Seminara, G., Zolezzi, G., Tubino, M., & Zardi, D. (2001). Downstream and upstream influence in river meandering. Part 2. Planimetric development. *Journal of Fluid Mechanics*, 438, 213–230. <https://doi.org/10.1017/S0022112001004281>
- Shen, Z., Aeschliman, M., & Conway, N. (2021). Paleodischarge reconstruction using oxbow lake sediments complicated by shifting hydrological connectivity. *Quaternary International*, 604(July), 75–81. <https://doi.org/10.1016/j.quaint.2021.07.004>
- Solari, L., Seminara, G., Lanzoni, S., Marani, M., & Rinaldo, A. (2002). Sand bars in tidal channels part 2. Tidal meanders. *Journal of Fluid Mechanics*, 451, 203–238. <https://doi.org/10.1017/s0022112001006565>
- Stølum, H. H. (1996). River meandering as a self-organization process. *Science*, 271(5256), 1710–1713. <https://doi.org/10.1126/science.271.5256.1710>
- Strick, R. J. P., Ashworth, P. J., Awcock, G., & Lewin, J. (2018). Morphology and spacing of river meander scrolls. *Geomorphology*, 310, 57–68. <https://doi.org/10.1016/j.geomorph.2018.03.005>
- Swartz, J. M., Goudge, T. A., & Mohrig, D. C. (2020). Quantifying coastal fluvial morphodynamics over the last 100 years on the lower Rio Grande, USA and Mexico. *Journal of Geophysical Research: Earth Surface*, 125(6), 1–16. <https://doi.org/10.1029/2019JF005443>
- Thomas, S. S., Constantine, J. A., Dethier, D., Thoman, J. W., Racela, J., Blau, E., & Landis, J. D. (2022). The importance of oxbow lakes in the floodplain storage of pollutants. *Geology*, 50(4), 392–396. <https://doi.org/10.1130/G49427.1>
- Toonen, W. H. J., Kleinhans, M. G., & Cohen, K. M. (2012). Sedimentary architecture of abandoned channel fills. *Earth Surface Processes and Landforms*, 37(4), 459–472. <https://doi.org/10.1002/esp.3189>
- Torres, M. A., Limaye, A. B., Ganti, V., Lamb, M. P., Joshua West, A., & Fischer, W. W. (2017). Model predictions of long-lived storage of organic carbon in river deposits. *Earth Surface Dynamics*, 5(4), 711–730. <https://doi.org/10.5194/esurf-5-711-2017>
- Turnipseed, C., Konsoer, K., Richards, D., & Willson, C. (2021). Numerical modeling of two-dimensional hydrodynamics in a highly curving and actively evolving neck cutoff under different hydrologic conditions. *Water Resources Research*, 57(2), 1–14. <https://doi.org/10.1029/2020WR027329>
- van de Lageweg, W. I., van Dijk, W. M., Baar, A. W., Rutten, J., & Kleinhans, M. G. (2014). Bank pull or bar push: What drives scroll-bar formation in meandering rivers? *Geology*, 42(4), 319–322. <https://doi.org/10.1130/G35192.1>
- Vermeulen, B., Hoitink, A. J. F., Zolezzi, G., Abad, J. D., & Aalto, R. (2016). Multiscale structure of meanders. *Geophysical Research Letters*, 43(7), 3288–3297. <https://doi.org/10.1002/2016GL068238>
- Vilas, F., Arche, A., Ferrero, M., & Isla, F. (1999). Subantarctic macrotidal flats, cheniers and beaches in San Sebastian Bay, Tierra Del Fuego, Argentina. *Marine Geology*, 160(3–4), 301–326. [https://doi.org/10.1016/S0025-3227\(99\)00021-3](https://doi.org/10.1016/S0025-3227(99)00021-3)
- Wu, C., Ullah, M. S., Lu, J., & Bhattacharya, J. P. (2016). Formation of point bars through rising and falling flood stages: Evidence from bar morphology, sediment transport and bed shear stress. *Sedimentology*, 63(6), 1458–1473. <https://doi.org/10.1111/sed.12269>
- Zhao, K., Coco, G., Gong, Z., Darby, S. E., Lanzoni, S., Xu, F., et al. (2022). A review on bank retreat: Mechanisms, observations, and modeling. *Reviews of Geophysics*, 60(2), 1–51. <https://doi.org/10.1029/2021rg000761>
- Zinger, J. A., Rhoads, B. L., & Best, J. L. (2011). Extreme sediment pulses generated by bend cutoffs along a large meandering river. *Nature Geoscience*, 4(10), 675–678. <https://doi.org/10.1038/ngeo1260>